An X-Ray Investigation of Carbonate Apatites

JAMES P. SMITH[1] and JAMES R. LEHR

Division of Chemical Development, Tennessee Valley Authority, Muscle Shoals, Ala.

Apatite, the principal mineral in commercial phosphate ores, varies widely in chemical reactivity and thermal stability. To correlate the mineralogical compositions of apatites with their reactivity, an x-ray study was made of the unit-cell dimensions of 55 samples of apatites from 47 domestic and foreign deposits; the samples represented nearly all commercially exploited deposits. The study was supported by petrographic and infrared examinations and by differential thermal analysis. The compositions of the apatites ranged from that of hydroxyapatite to that of francolite. When extraneous carbonate minerals were removed by a citrate extraction, refined lattice parameters, obtained from the x-ray data with a digital computer, showed that carbonate and fluorine substitute together for phosphate and cause significant changes in the apatite lattice, with concomitant increase in the chemical reactivity and decrease in the thermal stability of the apatite.

Apatite, the principal mineral in commercial phosphate ores, varies widely in chemical reactivity and thermal stability. This variation is reflected in differences among the ores in their behavior in acidulation processes by which they are converted to fertilizers. In an attempt to explain these differences, the apatite fractions of 55 phosphate rocks from 47 domestic and foreign sources were examined chemically and petrographically and by x-ray diffraction and infrared spectroscopy. Similar examinations were made of laboratory preparations of hydroxy- and fluorapatites.

Fluorapatite, the principal constituent of igneous phosphate deposits, occurs in massive, well-formed crystals with compositions close to that of $Ca_{10}(PO_4)_6F_2$ (*23*); its structure was determined independently by Naray-Szabo (*19*) and Mehmel (*18*). Hydroxyapatite, $Ca_{10}(PO_4)_6(OH)_2$, occurs only rarely in nature; the structure of hydroxyapatite was described by Posner, Perloff, and Diorio (*25*) who studied crystals prepared by a hydrothermal technique, and by Kay and Young (*12*) who examined natural crystals by x-ray and neutron study. The structure of hydroxyapatite is very similar to that of fluorapatite, for hydroxyl ions can occupy the sites of the fluoride ions on the sixfold axis.

The apatites in phosphorites and rock phosphates, however, are poorly crystallized and their compositions differ considerably from those of pure fluor- or hydroxyapatites, but their x-ray diffraction patterns are typically apatitic with slight shifts which show changes in the cell parameters. Most sedimentary phosphorites contain considerable amounts of carbonate (*23*) and are often considered carbonate apatites or francolite (*15*).

The literature on carbonate apatite is extensive and has been reviewed by McConnell (*15, 16*), Elliott (*6*), and others (*1, 3, 20, 28*). This literature contains much discussion of the validity of carbonate apatite as a true mineral species, but it is now generally agreed that carbonate substitutes for phosphate in the apatite lattice, although there is still disagreement on the details of this substitution. The length of the *a* axis varies with the carbonate content of the apatite (*17*), but no completely satisfactory correlation has been made between the unit-cell dimensions of carbonate apatites and their carbonate contents.

Sedimentary apatites almost always contain more fluorine in proportion to the phosphate than in the empirical formula $Ca_{10}(PO_4)_6F_2$, and the excess fluorine usually has been assumed to be present as calcium fluoride in crystals too small to be detected by x-ray. On the basis of chemical studies, however, Borneman-Starinkevitch and Belov (*2*) suggested that a carbonate ion replaces a phosphate ion in the apatite lattice, and that the vacant oxygen site is occupied by a fluoride ion. On this basis they postulated a series of solid solutions with the general composition $xCa_{10}(PO_4)_6F_2 + yCa_{10}(PO_4)_5CO_3(F, OH)_3$. Elliott (*6*) points out that this is the most convincing interpretation of the composition of carbonate apatites that has been advanced, even though a structure that requires close proximity of a fluoride and a carbonate ion is unusual.

Thus, there is substantial evidence that the planar carbonate ion substitutes in the apatite lattice for the tetrahedral phosphate ion; the triangle of oxygens of the CO_3 group then occupies the position of one face of the PO_4 tetrahedron that is replaced. The PO_4 tetrahedron is oriented so that two faces are parallel to the *c* axis and two are mutually inclined to the *c* axis. McConnell (*15*) postulated that the CO_3 group was parallel to the *c* axis. From the birefringence of carbonate apatite, Trautz (*30*) concluded that the substituted CO_3 group is inclined to the *c* axis, and Elliott (*6*) came to the same conclusion from polarized infrared studies.

Hendricks and Hill (*9, 10*) reported that "x-ray goniometer photographs of francolite" crystals are indistinguishable from those of apatite crystals, even in very high orders of diffraction, but they pointed out that replacement of phosphate by carbonate in the apatite structure should cause at least minor changes in the intensities of the reflections. Gruner and McConnell (*8*), however, found small but distinct changes in the intensities of certain francolite reflections from those of apatite reflections. Thus, very precise x-ray intensity data will be required to determine any differences between the structures of francolite and unsubstituted apatite.

In addition to refined x-ray techniques, careful preparation of samples of the mineral phosphates is required if the chemical compositions of the apatites are to be correlated with their unit-cell dimensions. When particle size permitted, the samples were sorted by hand under a low-power microscope to eliminate gangue minerals. Many of the apatites were contaminated with mechanically inseparable calcium and

[1] Deceased.

magnesium carbonates, and these were removed by extraction with citrate. Neither of these beneficiation methods was entirely successful, but they were sufficient to give apatite samples free enough of contaminants to permit estimation of the effect of the composition of carbonate apatites on their unit-cell dimensions when the results were treated statistically.

In addition to chemical analyses, this investigation was supported also by petrographic examinations, infrared spectroscopy, and differential thermal analyses.

X-Ray Methods

The powder diffraction data were obtained with a Norelco diffractometer equipped with a Philips high-intensity copper-target x-ray tube which was operated at 35 kv. and 15 ma. Essentially Cu$K\alpha$ radiation was obtained with nickel-foil filters. The width of the divergence and scatter slits was 1°; that of the receiving slit was 0.006 inch.

Determination of Lattice Constants. For the determination of lattice constants, line profiles were recorded at a scanning rate of 0.25° 2θ per minute over the angular range 25 to 54° 2θ; the time constant was 4 seconds, the chart speed 0.5 inch per minute. Continuous check on the instrument calibration was obtained by measuring the positions of a series of α-quartz lines, a convenient internal standard in most phosphate ores.

Interplanar spacings corresponding to the recorded reflections were calculated in the usual manner from Bragg's equation. The crystallites usually were so small that the α_1 α_2 doublet could not be resolved, and a weighted average of the two wavelengths was used, λ = 1.54178 A. With well-crystallized igneous phosphates, the value λ = 1.54050 A. was used.

For compounds such as apatite and α-quartz which can be referred to hexagonal axes, the relation between cell parameters a and c and any given interplanar spacing, d, of known Miller indices (hkl) is expressed by the equation

$$d_{hkl} = \frac{1}{\sqrt{\frac{4(h^2 + hk + k^2)}{3a^2} + \frac{l^2}{c^2}}} \quad (1)$$

Ten apatite reflections, corresponding to diffraction from the 300, 202, 310, 222, 312, 213, 321, 410, 402, and 004 sets of planes, were used in the refinement of the lattice constants of the francolites. The lattice constants of seven synthetic apatites (2 fluor-, 5 hydroxyapatites) were determined similarly; three of the apatites (F3, HY43H, and XP12H) were those used by Egan, Wakefield, and Elmore (*4*, *5*) in the determination of the thermodynamic properties of fluor- and hydroxyapatite.

Approximate values of a and c were inserted in Equation 1 to obtain a set of values of d_{hkl} corresponding to the observed d_{hkl} values obtained by measuring the peak positions of the line profiles. The cell parameters were refined by a least-squares method on a digital computer in which the calculated and observed values of d_{hkl} were converged until the corrections for values of a and c were decreased to the corresponding standard errors. A weighting factor, $1/d^2$, was introduced to minimize the influence of low-angle reflections on the solutions for values of a and c.

Determination of Crystallite Size. Approximate crystallite sizes were determined by the method of Rau (*26*). The line profiles of the 002 and the 300 reflections were obtained by scanning at a rate of 0.125° 2θ per minute, with a time constant of 8 seconds and a chart speed of 0.5 inch per minute. Since standards for crystallite-size measurements were not available, a sample of well-crystallized α-quartz was used to determine the widths at half-peak height of line profiles at Bragg angles of 35° or less. The values were in good agreement with those obtained by Rau for crystallite sizes 5000 A. and larger, and his crystallite-size curves were considered satisfactory for converting the experimental measurements to approximate crystallite sizes.

Chemical Methods

The phosphate rock samples are described in Table I. Each sample was prepared for analysis by repeated quartering and then grinding of the final portion to minus 200 mesh. The samples were analyzed both before and after the citrate extraction described below.

Table I. Apatite Concentrate Samples

No.	Source	Remarks
1	North Carolina	Flotation concentrate
2	North Carolina	Flotation concentrate
3	North Carolina	Phosphatized teeth and bone
4	South Carolina	Land rock concentrate
5	Morocco	60–100 mesh, mostly oolitic
6	Morocco	100–150 mesh, oolitic
7	Morocco	White oolitic fraction of concentrate
8	Morocco	Dull white fraction of concentrate
9	Morocco	Shipping concentrate
10	Morocco	Shipping concentrate
11	Morocco	Unground concentrate
12	Togo	Shipping concentrate
13	Gafsa	Shipping concentrate
14	Florida	White portion of 6–10 mesh concentrate
15	Florida	Gray portion of 6–10 mesh concentrate
16	Florida	Smooth white fraction of concentrate
17	Florida	Dull white fraction of concentrate
18	Florida	Land pebble shipping concentrate
19	Florida	Bone Valley phosphatized bone
20	Florida	Bone Valley phosphatized bone
21	Florida	Bone Valley phosphatized bone
22	Montana	Unbeneficiated ore
23	Montana	Douglas Creek Mine
24	Utah	Black phosphate rock
25	Wyoming	White phosphate rock
26	Wyoming	Phosphoric bed 4–28
27	Wyoming	Fish-scale phosphoria
28	Wyoming	Shipping concentrate
29	Tennessee	Brown plate rock
30	Tennessee	Plate rock, 65–100 mesh fraction
31	Tennessee	Plate rock, 100–150 mesh fraction
32	Tennessee	Plate rock, 150–200 mesh fraction
33	Tennessee	Plate rock, 14–20 mesh fraction
34	Tennessee	High-grade plate rock, 6–12 mesh
35	Tennessee	High-grade plate rock, 42–100 mesh
36	Baja California	Beach sand
37	Baja California	Beach sand concentrate
38	Peru	Shipping concentrate
39	Ocean Island	Shipping concentrate
40	Nauru Island	Shipping concentrate
41	Jordan	Green plate rock
42	Jordan	Ruseifa Mine, Amman
43	Jordan	High-grade concentrate
44	Quebec	Fluorapatite
45	Quebec	Fluorapatite
46	Quebec	Fluorapatite
47	Quebec	Fluorapatite
48	Quebec	Fluorapatite
49	Ontario	Fluorapatite
50	Ontario	Fluorapatite
51	Kola Peninsula	Fluorapatite
52	Kola Peninsula	Fluorapatite
53	Australia	Rum Valley deposit
54	Missouri	Igneous fluorapatite concentrate
55	Holly Springs, Ga.	Hydroxyapatite

Determinations were made of CaO, P_2O_5, F, and CO_2, which are the major constituents that account for most of the variations in the chemical and x-ray properties of the apatites. Calcium was determined volumetrically by the method of Kolthoff and Sandell (*13*), phosphorus gravimetrically as quinolinium molybdophosphate (*24*), fluorine by steam distillation with perchloric acid and titration with thorium nitrate to the purpurin sulfonate end point (*27, 31*), and carbon dioxide by evolution with perchloric acid and absorption on ascarite (*13*). The results are shown in Table II.

Citrate Extraction. Many of the samples contained free but mechanically inseparable calcium and magnesium carbonates which were removed by extraction with ammonium citrate solution. The less alkaline (pH 8.1) triammonium citrate solution of Silverman *et al.* (*28*) was more effective for this extraction than Petermann's alkaline (pH above 9) citrate solution (*21*).

The Silverman extraction procedure was modified to ensure maximum removal of calcite, aragonite, and dolomite from the phosphate samples. In the modified procedure, 1-gram portions of the minus 200-mesh samples were suspended in 100 ml. of 0.5*M* triammonium citrate solution (pH 8.1) and digested at 65° C. for 4 hours with constant agitation, after which the mixtures were allowed to stand at room temperature for 18 hours. The mixtures then were filtered, and the extracted samples were washed and dried at 105° C. The necessity for the longer extraction period was demonstrated by tests on eight samples that contained calcite, aragonite, and dolomite in different proportions, particle sizes, and amounts that could be determined by petrographic or infrared examination.

The applicability of the extraction procedure was tested by five successive extractions of a sample that initially contained free carbonates. Although the chemical composition of the residue was changed significantly by each extraction because of dissolution of small amounts of apatite, after the first extraction the relative amounts of CaO, P_2O_5, F, and CO_2 remained nearly constant, and there was no detectable change in the lattice constants of the apatite. As shown by the data in Table II, the extraction removed free carbonates and fluorides without effect on the x-ray characteristics of the apatite.

Minor Constituents. Results of spectrographic analyses of the extracted samples are shown in Table III. Silica, as quartz, clays, and feldspar, was the major contaminant of almost all the samples. A few samples contained small but significant amounts of aluminum present as aluminum phosphates. Most of the samples contained very small amounts of magnesium, barium,

Table II. Chemical Composition, Crystallite Size, and Unit-Cell

No.	Composition, % CaO	P_2O_5	F	CO_2	Crystallite Size, A. c (002)	a (300)	Cell Dimensions,[a] A. a_0	c_0
1	49.0	30.23	3.52	5.9	425	250	9.322	6.880
Extd.	49.4	31.11	3.74	5.3	...	...	9.315	6.883
2	48.3	30.27	3.64	5.2	480	280	9.324	6.888
Extd.	48.9	31.21	3.62	4.9	...	...	9.320	6.891
3	49.7	33.22	3.30	4.2	450	250	9.370	6.888
Extd.	50.0	34.48	3.46	2.9	...	...	9.368	6.884
4	44.9	28.26	3.75	4.9	1200	850	9.323	6.898
Extd.	44.3	27.69	3.63	4.9	...	...	9.322	6.899
5	52.3	32.80	4.4	5.3	700	330	9.326	6.895
Extd.	52.1	33.61	4.3	4.7	650	350	9.326	6.895
6	51.4	32.10	4.3	5.7	640	350	9.330	6.892
Extd.	51.7	32.96	4.10	5.0	...	...	9.324	6.892
7	51.2	30.80	3.85	7.4	900	550	9.331	6.901
Extd.	51.9	32.73	4.08	5.0	...	...	9.330	6.897
8	50.7	30.59	3.8	6.8	850	475	9.331	6.893
Extd.	51.1	32.88	4.0	4.6	880	430	9.334	6.895
9	51.5	33.01	4.19	4.4	700	390	9.332	6.892
Extd.	51.7	33.49	4.18	3.7	...	...	9.336	6.896
10	53.9	36.94	4.29	2.8	875	475	9.345	6.894
Extd.	53.9	37.18	4.29	2.3	...	...	9.347	6.895
11	52.2	32.46	4.19	5.8	850	600	9.327	6.891
Extd.	52.6	33.27	4.26	5.1	...	...	9.325	6.896
12	52.3	36.57	4.01	1.8	860	430	9.351	6.890
Extd.	52.7	37.00	4.04	1.7	...	...	9.351	6.894
13	48.0	29.12	3.52	6.1	700	380	9.324	6.894
Extd.	48.3	29.94	3.58	5.7	...	...	9.324	6.896
14	51.1	35.10	4.2	3.3	700	400	9.339	6.895
Extd.	51.2	35.08	4.2	3.4	700	440	9.337	6.895
15	50.3	34.60	4.1	3.2	700	440	9.336	6.895
Extd.	50.7	34.51	4.1	3.3	720	440	9.338	6.893
16	50.7	32.96	4.10	4.2	750	650	9.331	6.897
Extd.	51.0	32.38	4.02	4.1	...	...	9.331	6.897
17	49.0	31.94	3.7	4.8	760	600	9.330	6.896
Extd.	49.8	32.40	4.1	4.2	750	550	9.330	6.894
18	46.6	30.85	3.74	3.8	950	550	9.331	6.897
Extd.	46.1	30.36	3.74	3.9	...	...	9.328	6.901
19	50.5	36.59	3.20	3.6	480	230	9.360	6.890
Extd.	50.7	35.63	3.10	3.5	500	230	9.360	6.892
20	49.4	35.70	3.60	2.6	550	230	9.348	6.892
Extd.	51.6	37.32	3.70	2.8	480	240	9.348	6.892
21	49.4	37.09	3.30	2.9	450	225	9.359	5.890
Extd.	49.1	36.36	3.30	2.8	500	225	9.357	6.890
22	43.3	30.83	3.59	1.0	850	700	9.359	6.893
Extd.	44.0	31.62	3.54	1.1	...	...	9.359	6.892
23	43.7	27.41	2.93	7.1	750	750	9.362	6.889
Extd.	44.1	29.95	3.12	4.1	...	...	9.359	6.890
24	43.2	28.88	3.19	3.0	800	525	9.359	6.896
Extd.	44.1	30.66	3.38	1.9	...	...	9.358	6.895
25	44.5	31.14	3.32	1.6	900	620	9.364	6.890
Extd.	43.6	31.08	3.26	1.1	...	...	9.365	6.890
26	51.9	36.56	3.84	1.5	950	700	9.360	6.887
Extd.	51.8	36.71	3.60	1.7	...	...	9.360	6.890
27	46.5	32.00	3.62	1.9	1200	620	9.361	6.891
Extd.	45.8	32.16	3.60	1.6	...	...	9.362	6.891
28	47.0	29.64	3.87	2.9	900	600	9.355	6.886
Extd.	47.4	32.75	3.90	1.9	...	...	9.353	6.887
29	48.8	34.92	3.64	1.4	1100	700	9.358	6.891
Extd.	49.5	35.40	3.75	1.5	...	...	9.356	6.893

[a] The standard errors of a_0 and c_0 ranged only from 0.000 to 0.003 and were usually 0.001.
[b] Ignited at 950° C. for 2 hours in atmosphere containing 20% water vapor.

Dimensions of Apatite Concentrates before and after Extraction

No.	Composition, % CaO	P_2O_5	F	CO_2	Crystallite Size, A. c (002)	a (300)	Cell Dimensions,[a] A. a_0	c_0
30	45.4	35.56	3.65	0.9	950	800	9.361	6.892
Extd.	48.3	36.13	3.57	1.0	...	...	9.354	6.886
31	42.5	34.26	3.48	0.7	950	750	9.361	6.888
Extd.	46.0	34.98	3.49	0.8	...	...	9.354	6.885
32	41.1	33.52	3.46	0.7	1050	800	9.362	6.888
Extd.	43.7	34.21	3.37	1.1	...	...	9.352	6.886
33	42.9	34.77	3.71	0.8	950	800	9.363	6.890
Extd.	46.3	35.55	3.67	0.9	...	...	9.351	6.885
34	52.2	35.77	4.12	2.7	1200	850	9.347	6.894
Extd.	52.7	36.04	3.97	2.6	...	...	9.349	6.893
35	51.9	35.45	3.89	2.4	1200	800	9.347	6.896
Extd.	51.5	35.93	3.96	2.8	...	...	9.348	6.893
36	46.0	29.96	3.26	4.5	500	300	9.338	6.888
Extd.	45.9	30.40	3.19	4.0	...	...	9.341	6.884
37	46.9	29.06	3.25	5.9	580	230	9.336	6.889
Extd.	45.5	30.47	3.27	4.3	...	...	9.337	6.884
38	46.3	30.45	3.07	4.3	580	236	9.338	6.887
Extd.	46.8	31.30	3.07	4.5	...	...	9.337	6.886
39	53.0	39.65	2.84	1.4	800	550	9.378	6.885
Extd.	53.2	39.82	2.91	1.2	...	...	9.377	6.886
40	52.9	38.67	2.50	2.2	850	400	9.377	6.890
Extd.	53.0	38.74	2.56	2.1	...	...	9.378	6.893
41	55.9	38.07	3.55	1.5	>2000	...	9.364	6.891
Extd.	55.8	37.99	3.97	1.8	...	...	9.358	6.892
42	40.9	26.68	3.19	3.3	780	400	9.336	6.898
Extd.	40.0	26.31	3.18	2.9	...	...	9.332	6.897
43	53.0	33.77	4.05	4.9	630	400	9.333	6.899
Extd.	52.4	34.35	4.29	4.2	...	...	9.332	6.896
44	55.5	40.52	3.38	0.3	>2000	...	9.378	6.886
Extd.	55.5	40.55	3.42	0.4	...	...	9.384	6.886
45	53.8	39.97	3.16	0.2	>2000	...	9.374	6.883
Extd.	54.5	40.04	3.28	0.3	...	...	9.372	6.883
46	55.1	39.54	2.82	0.4	>2000	...	9.389	6.882
Extd.	55.0	39.72	2.82	0.3	...	...	9.386	6.882
47	55.3	39.82	3.24	0.5	>2000	...	9.371	6.879
Extd.	54.8	39.95	3.30	0.4	...	...	9.375	6.885
48	55.8	40.53	3.15	0.3	>2000	...	9.367	6.880
Extd.	54.9	40.55	3.22	0.4	...	...	9.370	6.885
49	52.3	36.46	2.90	0.5	>2000	...	9.399	6.901
Extd.	52.3	37.02	2.60	0.4	...	...	9.399	6.901
50	55.4	42.13	3.80	0.8	>2000	...	9.362	6.884
Extd.	55.0	40.75	3.56	0.7	...	...	9.363	6.884
51	51.4	38.34	3.10	>0.1	>2000	...	9.383	6.887
Extd.	51.9	38.75	3.21	0.3	...	...	9.382	6.887
52	52.2	39.00	3.20	0.2	>2000	...	9.384	6.890
Extd.	53.0	39.09	2.76	0.3	...	...	9.383	6.893
53	52.3	39.27	3.58	0.3	>2000	...	9.370	6.881
Extd.	53.1	39.55	3.70	0.3	...	...	9.369	6.883
54	51.0	35.04	3.54	3.0	>2000	...	9.368	6.878
Extd.	51.1	37.88	3.88	0.3	...	...	9.368	6.876
55	54.5	42.2	...	...	...	...	9.422	6.874
Synthetic Fluorapatite								
31e	55.7	42.3	3.65	...	...	...	9.367	6.882
F-3	55.6	42.2	3.75	...	...	...	9.367	6.882
Stoichiometric	55.60	42.22	3.77	...	...	...	...	...
Synthetic Hydroxyapatite								
HY-43	55.17	41.62	...	...	...	...	9.420	6.878
HY-43-H[b]	55.70	42.35	...	...	...	...	9.414	6.878
HY-42	55.75	42.41	...	...	...	...	9.415	6.874
XP12H[b]	55.71	42.32	...	...	...	...	9.415	6.878
HA-2	55.79	42.39	...	0.0	...	...	9.415	6.877
Stoichiometric	55.80	42.39	...	...	...	...	...	...

and strontium which can substitute for calcium, but the amounts of these elements usually were small enough to be ignored. Samples containing the largest amounts of magnesium, however, were shown petrographically to contain dolomite that was not removed completely by the citrate extraction. Another phase of this investigation showed that some of the magnesium and iron was associated with the organic matter present in the phosphate ore.

Results

In correlations of the unit-cell parameters of the apatites with their chemical compositions, the amounts of PO_4, F, and CO_3 were expressed as moles per 10 moles Ca for comparison with the accepted formula for fluorapatite, $Ca_{10}(PO_4)_6F_2$.

Previous investigators have usually attributed changes in the unit-cell parameters of the apatites in phosphate ores to the effects of substitution in the lattice of either fluorine alone or carbonate alone. The separate effects of these constituents are shown in Figures 1 and 2.

As shown in Figure 1, there is a reasonable correlation between the total fluorine content and the length of the *a* axis, but the data scatter considerably, and the line of best fit extrapolates to a value far above 9.42 A., the length of the *a* axis in hydroxyapatite. As shown in Figure 2, there is also a reasonable correlation between the carbonate content and the length of the *a* axis, but the data scatter considerably at low carbonate contents, and the line of best fit extrapolates to 9.376 A., a value close to that, 9.37 A., for the *a* axis in fluorapatite. Although the correlation with carbonate appears better than that with fluorine, neither constituent alone explains satisfactorily the changes in the apatite lattice.

The additive effects of fluorine and carbonate, however, correlate well with the changes in the length of the *a* axis, as shown in Figure 3. Two of the points farthest from the line of best fit are those for samples containing constituents that either distort the chemical composition (No. 23 contains microscopically coarse free dolomite that resisted the citrate extraction) or significantly affect the lattice parameters (No. 49, an igneous apatite, contains significant amounts of rare earths and strontium, elements known to alter the length of the *a* axis).

The solid line of best fit for the natural apatites in Figure 3 extrapolates to a length of the *a* axis very close to that in hydroxyapatite; the dashed line is drawn through compositions of synthetic apatites in which only fluorine substitution is involved. Although the differences in slope and position of the two lines of best fit for the natural and synthetic apatites are appreciable, they

Table III. Minor Constituents of Apatite Concentrates

Order of magnitude determined spectrographically; values determined chemically are in parentheses

No.	Composition, %[a]									Rare Earths[b]	
	SiO_2	MgO	Al_2O_3	Fe_2O_3	Na_2O	K_2O	SrO	BaO	Cr_2O_3	Yb	Y
1	3	0.5	0.7	0.7	...	...	0.2	0.05	0.02	P	P+
2	3	0.5	0.7	0.5	...	...	0.2	0.1	0.03	P+	P+
3	1	0.3	0.1	0.5	...	...	0.2	0.01	0.001	P	P
4	10	0.5	1	1	...	...	0.1	0.1	0.01	P	P+
5	(0.64)	(0.38)	(0.25)	(0.11)	(1.28)	(0.02)	0.1	0.05	0.03	P	P
6	1.5	0.4	0.3	0.1	...	...	0.1	0.05	0.03	P	P
7	3	0.5	0.3	0.1	...	...	0.1	0.05	0.02	P	P
8	(2.57)	(0.51)	(0.21)	(0.14)	(0.77)	(0.04)	0.1	0.05	0.02	P	P
9	2	0.3	0.2	0.1	...	...	0.1	0.05	0.03	P	P
10	2	0.2	0.2	0.2	...	...	0.05	0.03	0.02	P	P
11	1	0.3	0.1	0.1	...	...	0.1	0.05	0.02	P	P
12	2	0.2	0.3	1	...	...	0.05	0.05	<0.01	P	P
13	2	0.4	0.2	0.2	...	...	0.2	0.01	0.02	P	P
14	(1.71)	(0.17)	(0.72)	(0.36)	(0.73)	(0.04)	0.1	0.02	0.01	P	P
15	(3.21)	(0.17)	(1.36)	(0.36)	(0.65)	(0.04)	0.1	0.02	0.01	P	P
17	(3.00)	(0.41)	(0.68)	(0.92)	(0.80)	(0.06)	<0.1	0.01	0.001	P	P
18	10	0.5	1	2	...	...	0.1	0.05	0.01	P	P
19	(0.20)	(0.12)	(1.19)	(0.53)	(0.57)	(<0.01)	0.1	0.01	0.01	n.d.	n.d.
20	(0.20)	(0.25)	(0.96)	(0.50)	(0.82)	(<0.01)	0.1	0.5	0.005	n.d.	n.d.
21	(<0.2)	(0.15)	(0.83)	(0.27)	(0.92)	(0.01)	0.1	0.05	0.005	P−	P−
22	10	0.1	0.8	0.8	...	...	0.1	0.1	0.02	P	P
23	10	1	1	0.8	...	...	0.1	0.1	0.05	P+	P
24	10	0.5	1	0.5	...	...	0.1	0.05	0.05	P	P
25	10	0.2	1	1	...	...	0.1	0.1	0.05	P+	P+
26	2	0.2	0.5	1	...	...	0.05	0.05	0.05	P	P
27	5	0.4	0.8	0.2	...	...	0.1	0.1	0.1	P+	P+
28	7	0.3	1	0.5	...	...	0.2	0.05	0.5	P+	P+
29	3	0.1	1	2	...	...	0.05	0.01	0.001	P	P
30	3	0.2	3	2	...	...	0.05	0.1	<0.001	P	P
31	3	0.2	3	2	...	...	0.05	0.1	<0.001	P	P
32	3	0.2	3	0.8	...	...	0.05	0.01	0.001	P	P+
33	3	0.2	3	2	...	...	0.05	0.1	<0.001	P	P
34	3	0.1	0.8	1	...	...	0.05	0.05	n.d.	P	P
35	3	0.1	0.8	1	...	...	0.05	0.05	<0.01	P	P
36	3	0.5	2	2	...	...	0.2	0.1	0.05	P	P
37	7	0.8	2	3	...	...	0.2	0.1	0.02	P	P−
38	3	0.5	1	0.5	...	...	0.2	0.05	0.01	P	P
39	0.5	0.2	0.1	0.2	...	...	0.05	0.05	0.001	n.d.	n.d.
40	0.2	0.3	0.3	0.5	...	...	0.05	0.01	0.01	n.d.	n.d.
41	1	0.1	0.1	0.2	...	...	0.1	0.05	0.01	P	P
42	8	0.2	0.2	<0.1	...	...	0.1	0.05	0.01	P	P
43	2	0.1	0.1	0.05	...	...	0.2	0.1	0.01	P	P−
44	0.5	0.2	<0.1	0.1	...	...	0.2	n.d.	0.01	P	P
45	2	0.1	0.1	0.5–0.8	...	...	0.2	<0.01	n.d.	P+	P−
46	1	<0.05	<0.1	<0.1	...	...	0.2	n.d.	n.d.	P	P
47	0.3	0.05	<0.1	<0.1	...	...	0.2	n.d.	n.d.	n.d.	P−
48	1	0.05	<0.1	<0.1	...	...	0.2	n.d.	n.d.	P	P
49	3	0.2	<0.1	2	...	...	0.5	0.5	n.d.	P+	P+
50	0.3	<0.05	<0.1	0.1	...	...	0.1	n.d.	n.d.	P++	P++
51	2	0.1	0.5	0.5	...	...	0.2	0.2	n.d.	P	P+
52	2	0.1	0.5–0.7	1	...	...	0.5	0.2	0.01	P+	P−
53	2	0.1	2	2	...	...	<0.01	<0.01	0.01	n.d.	P
54	2	0.5	0.3	2	...	...	0.05	0.2	n.d.	P+	P+
55	1	0.5	<0.1	0.2	...	...	0.02	n.d.	0.001	P	P

[a] n.d. = not detected.
[b] P = present, + and − indicate larger or smaller amounts than usual.

Table IV. Mathematical Correlation of Axis Lengths with Chemical Composition[a]

	Model	Constants				Standard Error				
		a_{00} or c_{00}	b	c	d	a_{00} or c_{00}	b	c	d	$a_0 - a_o$ or $c_0 - c_c$
1	$a_0 = a_{00} + bF$	9.464	−0.053	...	...	0.015	0.007	...	...	0.013
2	$a_0 = a_{00} + bC$	9.376	−0.039	...	...	0.002	0.003	...	...	0.009
3	$a_0 = a_{00} + b(F + C)$	9.433	−0.030	...	...	0.004	0.001	...	...	0.006
4	$a_0 = a_{00} + bF + cC$	9.430	−0.028	−0.030	...	0.008	0.004	0.002	...	0.006
5	$a_0 = a_{00} + bF + cC + dFC$	9.420	−0.023	−0.005	0.021	0.012	0.006	0.021	0.010	0.006
1c	$c_0 = c_{00} + bF$	6.896	0.010	...	...	0.006	0.003	...	...	0.005
2c	$c_0 = c_{00} + bC$	6.886	0.006	...	...	0.001	0.002	...	...	0.005
3c	$c_0 = c_{00} + b(F + C)$	6.876	0.005	...	...	0.003	0.001	...	...	0.005
4c	$c_0 = c_{00} + bF + cC$	6.874	0.006	0.005	...	0.006	0.003	0.002	...	0.005
5c	$c_0 = c_{00} + bF + cC + dFC$	6.888	0.000	−0.027	0.015	0.009	0.014	0.015	0.007	0.005

[a] $a_0(c_0)$ = observed length of $a(c)$ axis, A. $a_{00}(c_{00})$ = limiting length of $a(c)$ axis, A. $a_c(c_c)$ = length of $a(c)$ axis, A., calculated from model. F = moles F/10 moles Ca. C = moles CO_3/10 moles Ca.

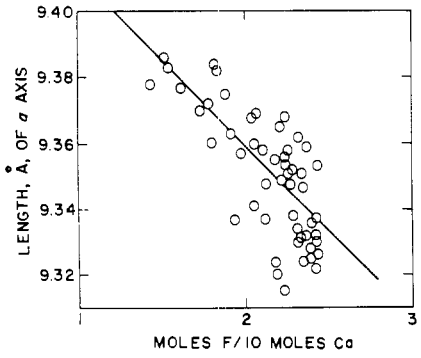

Figure 1. Effect of fluorine on length of a axis

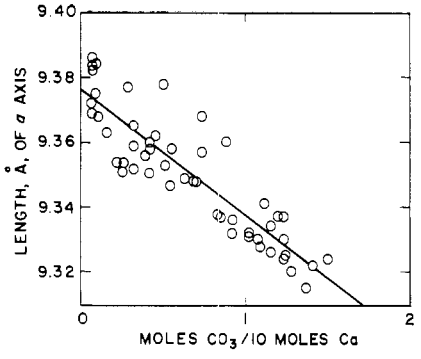

Figure 2. Effect of carbonate on length of a axis

probably are within the limits of experimental error.

The necessity for the citrate extraction is shown by Figure 4 in which the compositions of the unextracted samples are plotted with the line of best fit for the natural apatites from Figure 3. The directions in change in composition resulting from the citrate extraction are indicated by the arrows; most of the changes, resulting from removal of free carbonates, moved the compositions closer to the line of best fit.

Changes in composition of the apatites are reflected in changes in the length of the *c* axis also, as shown in Figure 5, but the effect is much less than that on the *a* axis. The accepted value for the length of the *c* axis in both hydroxy- and fluorapatite is 6.88 A.

The scatter of the data in the correlations of unit-cell parameters with chemical composition in Figures 3 and 5 result from two sources of experimental error, one of which is in the composition and the other in the measured x-ray parameters. In the compositions of the extracted samples, the small amounts of impurities were ignored; most of these impurities were constituents of gangue minerals (quartz, clays, and hydrous oxides of iron and aluminum), but in some samples dolomite and free calcium fluoride resisted the citrate extraction, and some of the impurity elements probably had substituted in the apatite lattice. Although the lattice parameters were obtained under highly reproducible conditions, variations in the linear absorption coefficients and crystallite sizes of the apatites probably introduced small errors.

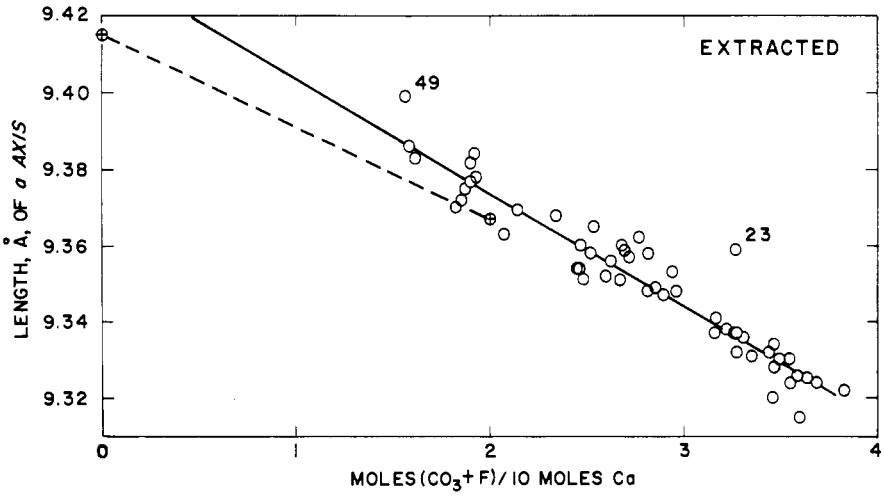

Figure 3. Effect of fluorine plus carbonate on length of a axis

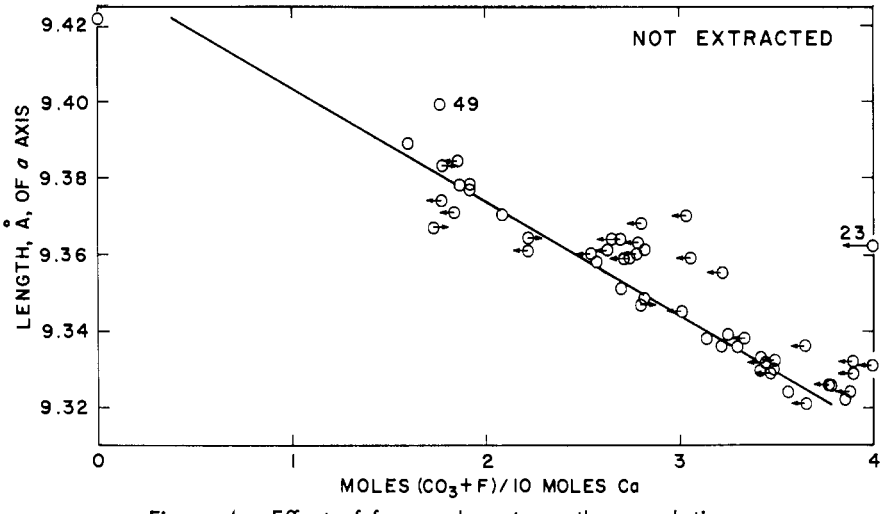

Figure 4. Effect of free carbonate on the correlation

Arrows show direction of shift when free carbonates are removed

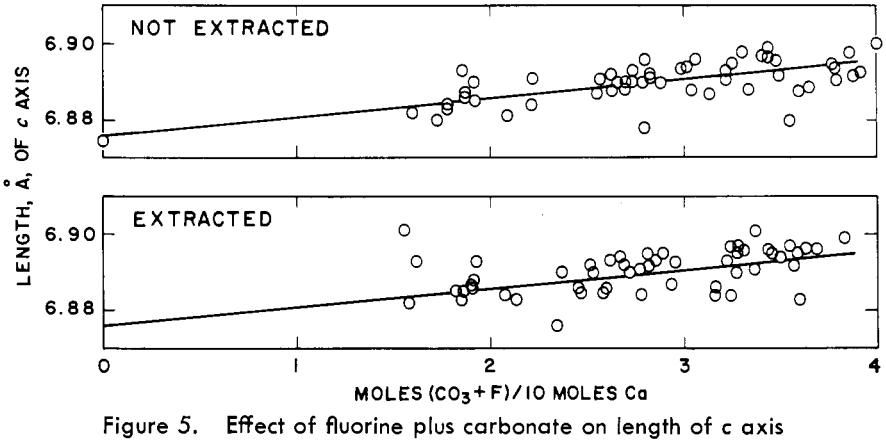

Figure 5. Effect of fluorine plus carbonate on length of c axis

Since both the compositional and mensuration errors are difficult to evaluate, the data were evaluated statistically by determination of their fit to five different models, three of which are illustrated in Figures 1, 2, and 3. All the models are described mathematically in Table IV, and the test was a least-squares regression analysis programmed for a digital computer. In Model 1 of Table IV, for example, a_0 is the observed length of the *a* axis, F is the fluorine content in moles F per 10 moles

Ca, b is the slope of line of best fit of the observed lengths of the a axis for all the experimental points, and the standard error of $a_0 - a_c$ is a measure of the agreement of the calculated values with the observed values.

Models 1, 2, and 3 are mathematical expressions of the best-fit lines in Figures 1, 2, and 3, respectively. Model 3, with the smallest standard error of $a_0 - a_c$, gives the best fit to the data and extrapolates to a value of a_{00} of 9.433 A. which is close to the length of the a axis in hydroxyapatite. Use of different coefficients to express the separate effects of fluorine and carbonate, as in Model 4, or addition of a term for the interaction of fluorine and carbonate, as in Model 5 makes no improvement in the fit.

Similar mathematical treatment of the data to explain the relation between chemical composition and the length of the c axis showed also that the best fit was obtained when the effects of fluorine and carbonate were considered equal and additive, as in Model 3c of Table IV.

Since one carbonate group substitutes for one phosphate group in the apatite lattice, the plot of the moles of phosphate against moles of carbonate, as in Figure 6, should be a straight line with slope of -1, as indicated by the dashed line. Although several of the compositions fall close to this line, the best fit to the data, the solid line in Figure 6, has a slope of -0.66 mole PO_4 per mole CO_3 and extrapolates to 5.90 ± 0.03 mole PO_4 per 10 moles Ca at zero carbonate.

As the small amounts of residual free dolomite and calcite were insufficient to account for the discrepancy in Figure 6, it was concluded that the discrepancy reflected the presence of nonapatitic phosphates. For example, samples 30 to 33 (designated by triangles in Figure 6) were shown petrographically and by x-ray to contain wavellite in amounts that account well for the distances of these points from the theoretical lines, and wavellite has been found in several of the other samples. Complex aluminum phosphates, such as millisite, crandallite (*11*), and wavellite (*22*) are reported to be formed by supergene alteration of the apatite in the upper strata of the Florida Bone Valley formation, and similar alterations are to be expected in other shallow sedimentary phosphate deposits. Further study is being made of the accessory minerals in the phosphate samples.

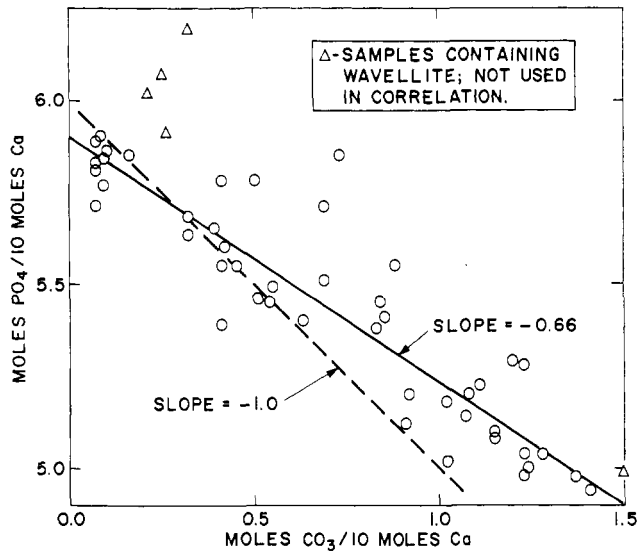

Figure 6. Relation between phosphate and carbonate in substituted apatites

Thermal Stability

Calcination of phosphate ores upgrades the ores by decomposition of the organic matter and volatilization of the adsorbed moisture and most of the combined carbon dioxide. Loss of carbon dioxide results in changes in the apatite unit-cell dimensions (*3*, *17*) and differential thermal analysis showed exothermic effects with francolites that are not observed with either fluor- or hydroxyapatite. A study was made of the effect of calcination for 1 hour in air on the carbonate apatite in a Florida phosphate (sample 14) and a Morocco phosphate (sample 5). The calcined samples were analyzed chemically and examined by x-ray to determine the crystallite size and the unit-cell parameters of the residual apatite. The results are shown in Table V.

The major effect of calcination of these carbonate apatites was evolution of carbon dioxide with consequent increase in crystallite size and recrystallization as fluorapatite—the lengths of both the a and c axes approached those in pure fluorapatite. The loss of carbon dioxide resulted in the formation and segregation of granular isotropic calcium oxide and sometimes small amounts of dendritic calcium fluoride from reaction of liberated fluorine with the calcium oxide. Both these products were detected petrographically in residues that had been calcined at 800° C. or above.

The effect of the loss of carbon dioxide on the length of the a axis in the residual apatite is shown in Figure 7 in which the effect of fluorine is ignored. The slopes of the two lines, -0.036 for sample 14 and -0.037 for sample 5, are nearly identical and are in close agreement with that, -0.039, obtained for Model 2 in Table IV in which the effect of fluorine also was ignored. In his studies of

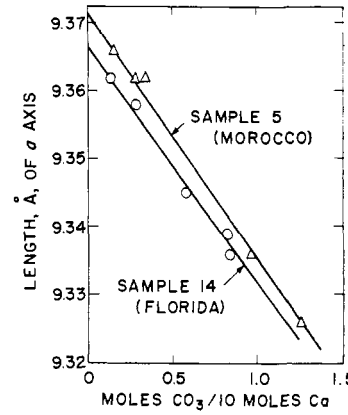

Figure 7. Effect of removal of carbonate from substituted apatites on length of a axis

Table V. Effect of Calcination on Substituted Apatites

Sample No.	Temp., ° C. of Calcination	Composition, % CaO	P_2O_5	F	CO_2	Ign. loss	Crystallite Size, A. (300)	Unit-Cell Dimensions, A.[a] a_0	c_0
14	Initial	51.1	35.1	4.2	3.3	...	500	9.339	6.895
	600	53.1	35.9	4.3	3.5	2.3	500	9.336	6.889
	750	54.0	36.6	4.2	2.5	3.7	600	9.345	6.889
	850	54.8	37.1	4.4	1.2	5.1	1200	9.358	6.889
	1050	55.0	37.4	4.4	0.6	6.0	2500	9.362	6.880
5	Initial	52.3	32.8	4.4	5.3	...	300	9.326	6.895
	600	57.3	34.5	4.2	4.3	3.6	300	9.336	6.897
	750	59.1	35.6	4.6	1.6	6.7	700	9.362	6.891
	850	59.2	35.7	4.5	1.3	7.1	1400	9.362	6.885
	1050	59.8	35.9	4.5	0.7	7.7	2500	9.366	6.888

[a] The standard error of a_0 and c_0 ranged only from 0.001 to 0.002.

francolites, Trautz (*29*) also reported a decrease in the length of the *a* axis of 0.039 A. per mole CO_2 when the composition was expressed on the basis of 10 moles Ca and the effect of fluorine was ignored.

The removal of carbon dioxide by calcination of carbonate apatites results in concomitant loss of excess fluorine and recrystallization of stoichiometric fluorapatite. This recrystallization to a more stable apatite results in increased cyrstallite size and decreased internal surface; these factors account for the decrease in reactivity on calcination that was observed by Freeman, Caro, and Heinly (*7*).

Conclusions

The fluorine in phosphorites in excess of that required to fill the hexad sites in the apatite lattice has usually been considered to be present as associated calcium fluoride that exists in undetectably small particles. This excess fluorine appears to enter the apatite lattice along with carbonate with consequent change of the unit-cell dimensions. Substitution of a divalent planar carbonate group for a trivalent tetrahedral phosphate group creates a charge imbalance and a packing void; addition of a fluoride (or hydroxyl) ion would preserve both the tetrahedral symmetry and the charge of the replaced phosphate group. Since there would be no coupling between the carbonate and fluoride ions in the hypothetical tetrahedral unit thus formed, either ion would be free to occupy the site vacated by the phosphate ion; although the manner of insertion of the carbonate ion could tend to block the entry of the fluorine, in the ideal arrangement one fluorine would substitute with one carbonate. The mole ratios of excess fluorine to carbonate in the samples examined, however, indicate that only one-third to one-half of the possible substitution sites are occupied by fluorine.

As shown by x-ray examinations, dual substitution of carbonate and fluoride for phosphate results in regular changes in the unit-cell dimensions of the apatite.

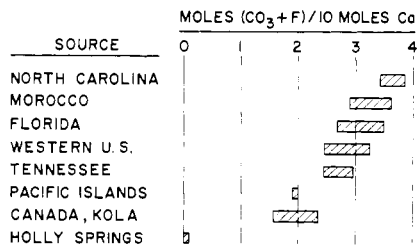

Figure 8. Correlation of chemical reactivity of apatites with degree of substitution

These changes are reflected also in regular changes in the optical properties and infrared spectra which will be reported later. In addition, substitution of carbonate and fluorine for phosphate in the apatite lattice increases the chemical reactivity of the apatite, as is shown qualitatively in Figure 8 in which commercially exploited phosphate ores from different deposits are listed in descending order of their reactivity in acidulation processes. The most highly substituted phosphates are those from Morocco and North Carolina, and these are also the most reactive. Phosphorites in which there has been less substitution, such as Kola phosphates, are markedly less reactive. The relation between chemical reactivity and degree of substitution is being studied further.

Literature Cited

(1) Ames, L. L., *Econ. Geol.* **54,** 829–41 (1959).
(2) Borneman-Starinkevitch, I. D., Belov, N. N., *Dokl. Akad. Nauk SSSR* **90,** 89–92 (1953).
(3) Carlström, D., *Acta Radiol. Suppl.* **121,** 59 pp. (1955).
(4) Egan, E. P., Jr., Wakefield, Z. T., Elmore, K. L., *J. Am. Chem. Soc.* **72,** 2418–21 (1950).
(5) *Ibid.*, **73,** 5581–2 (1951).
(6) Elliott, J. C., doctoral thesis, University of London, May 1964.
(7) Freeman, H. P., Caro, J. H., Heinly, N., J. Agr. Food Chem. **12,** 479–86 (1964).
(8) Gruner, J. W., McConnell, D., *Z. Krist.* **97,** 208–15 (1937).
(9) Hendricks, S. B., *Trans. Macy Conf.* **4,** 185–212 (1952).
(10) Hendricks, S. B., Hill, W. L., *Proc. Natl. Acad. Sci.* **36,** 731–7 (1950).
(11) Hill, W. L., Armiger, W. H., Gooch, S. D., *Mining Eng.* **187,** 699–702 (1950).
(12) Kay, M. I., Young, R. A., *Nature* **204,** 1050–2 (1964).
(13) Kolthoff, I. M., Sandell, E. B., "Textbook of Quantitative Inorganic Analyses," 3rd ed., pp. 370–75, 564, MacMillan, New York, 1952.
(14) McConnell, D., *Econ. Geol.* **53,** 110–11 (1958).
(15) McConnell, D., *J. Dental Research* **31,** 53–63 (1952).
(16) McConnell, D., *Science* **136,** 241–4 (1962).
(17) Maslennikov, B. M., Kavitskaya, F. A., *Dokl. Akad. Nauk SSSR* **109,** 990–2 (1956).
(18) Mehmel, M., *Z. Phys. Chem.* **15,** 223–41 (1931).
(19) Naray-Szabo, St., *Z. Krist.* **75,** 387–98 (1930).
(20) Neuman, W. F., Neuman, M. W., *Chem. Rev.* **53,** 1–45 (1953).
(21) Organization for European Economic Co-operation, *Methods of Analysis Used in OEEC Countries*, pp. 82–3, Paris, 1952.
(22) Owens, J. P., Altschuler, Z. S., Berman, R., *Am. Mineralogist* **45,** 547–61 (1960).
(23) Palache, C., Berman, H., Frondel, C., "Dana's System of Mineralogy," Vol. **II,** pp. 877–89, Wiley, New York, 1951.
(24) Perrin, C. H., *J. Assoc. Offic. Agr. Chemists* **41,** 758–63 (1958).
(25) Posner, A. S., Perloff, A., Diorio, A. F., *Acta Cryst.* **11,** 308–9 (1958).
(26) Rau, R. C., "Advances in X-Ray Analyses," Vol. **5,** pp. 104–116, Univ. of Denver, Plenum Press, New York, 1962.
(27) Reynolds, D. S., Hill, W. L., *Ind. Eng. Chem., Anal. Ed.* **11,** 21–7 (1939).
(28) Silverman, S. R., Fuyat, R. K., Weiser, J. D., *Am. Mineralogist* **37,** 211–22 (1952).
(29) Trautz, O. R., *Ann. N. Y. Acad. Sci.* **60,** 696–712 (1955).
(30) *Ibid.*, **85,** 145–60 (1960).
(31) Willard, H. H., Horton, C. A., *Anal. Chem.* **22,** 1190–4 (1950).

Received for review February 14, 1966. Accepted May 23, 1966.